JOURNAL OF MATERIALS SCIENCE **36** (2001) 5633–5641

Laser-induced surface acoustic waves for evaluation of elastic stiffness of plasma sprayed materials

X. Q. MA*,‡, Y. MIZUTANI, M. TAKEMOTO
Faculty of Science and Engineering, Aoyama Gakuin University, Tokyo 157, Japan
E-mail: ma03161995@yahoo.com; ma@mat.ensmp.fr

The elastic properties of plasma sprayed deposits have been evaluated using a laser-excited surface acoustic wave (SAW) technique and an inversion processing analysis. The SAWs including Lamb and Rayleigh waves were generated in plasma sprayed NiCoCrAlY and ZrO_2, respectively, and their group velocity dispersions were used to determine the elastic properties (i.e.Young's modulus, Poison's ratio and density) of the deposits. Estimated elastic moduli from the velocity dispersions of A_0-mode Lamb waves are in the range of 40–140 GPa for the deposits, which are much lower than the values 220–240 GPa of the comparable dense materials. The dramatic reductions in modulus and density of ZrO_2 deposit have been attributed to the presence of high porosity and particularly microcracks. Moreover, this study has emphasized on exploiting the applicability of each kind of the SAWs for the elastic property evaluation of different sprayed materials. Both Lamb and Rayleigh wave dispersions are useful for the estimation of APS and VPS-deposited NiCrAlY, but S_0-Lamb and Rayleigh waves are exceptional for that of sprayed ZrO_2, because of its characterization of high acoustic attenuation and inconsequent displacement across the weak bonded interface of ZrO_2 and substrate.

1. Introduction

Elastic properties of materials are of considerable importance in determining their mechanical and thermomechanical behavior, especially fracture behavior. In comparison to bulk materials, thermal sprayed materials have a characterization of inhomogeneous composition (unmelted particle and oxide inclusions) and defective microstructures (crack, pore and lamellar splat), so their elastic properties can not be referred to the existing values of the bulk materials in literature. Some conventional test techniques such as tensile, bending and cantilever tests, have been used for measuring elastic properties of sprayed materials, but the experimental data always were quite dispersive among the tests and the methods [1–3], primarily because of a high sensitivity to local defects. For example, the Young's modulus of partially yttria-stabilized zirconia varies in the range of 10–100 GPa, depending on the coating processes and the measurement methods. Moreover, some local measurement methods such as micro-indentation test have been developed to overcome the difficulty of large-size sample required in conventional mechanical tests, and permit to measure Young's modulus in a local region of the deposits, but also contribute to a large scattering of data due to the inhomogeneous composition and microstructure [4–6]. Therefore, the experimental methods and the theoretical algorithms for accurate evaluation of overall elastic properties of sprayed materials are necessary to be developed.

Nondestructive ultrasonic techniques such as pulse-echo or through transmission methods have been widely used to determine elastic constants of variety of materials [7–9]. In practice, it is difficult to measure the elastic properties of thin films or coatings by conventional ultrasonic techniques, but surface acoustic waves (SAWs) which propagate in the surface layer have been useful [10–14]. In SAW technique, SAWs are excited and received at a comparable long propagation length to film thickness, and so the received SAWs contain an overall physical characterization of the tested material, and therefore a good reproducible results can be obtained through reducing the detection sensitivity to local defects in porous deposits. The elastic properties of porous silicon films were obtained from the phase velocity dispersion of Rayleigh waves and those of a plasma sprayed metallic coating from the group velocity dispersion of Rayleigh wave [15–17]. This latter technique is attractive for nondestructive

*Author to whom all correspondence should be addressed.
‡*Present Address*: Centre des Materiaux P.M. Fourt, B.P.87-91003 Evry CEDEX France.

inspection application, however, when the coating is porous and severely microcracking, this approach has been unsuccessful. For SAW techniques, the laser ultrasonic techniques were developed rapidly and applied to SAWs' generation and monitoring [18–20]. One advantage of laser ultrasonic technique over traditional one is noncontact, totally avoiding the use of liquid couple medium such as water, which is believed to have a negative influence on the estimated properties of porous materials due to the liquid impingement into the opening surface pores in conventional ultrasonic techniques.

In this study, SAWs including Lamb and Rayleigh waves were induced and monitored by a laser ultrasonic and interferometer system. The elastic properties of plasma sprayed thermal barrier coatings (TBCs) were evaluated in a procedure of Simplex-based inversion processing using the group velocity dispersions of Lamb waves for freestanding films of NiCoCrAlY and ZrO_2-Y_2O_3, and those of Rayleigh waves for coated steel samples. In addition, the applicability of group velocity dispersions of several mode SAWs for the elastic property estimation of sprayed deposits were investigated by correlating the acoustic properties to their microstructures.

2. Experimental procedure

Experiments were carried out on three kinds of plasma sprayed materials. AISI304 stainless steel of 10 mm thick were used as substrates, and were grit blasted with Al_2O_3 (700 μm), degreased and cleansed with alcohol prior to spraying. NiCoCrAlTaY (AMDRY 997, Sulzer Metco) was deposited by both atmospheric plasma spraying (APS) and vacuum plasma spraying (VPS). ZrO_2-8%Y_2O_3 (ZRO-178, Praxair) was deposited by APS processing. Plasma spray parameters are given in Table I. In order to prepare freestanding films, the coatings were sprayed onto a thin and fine polished stainless steel sheet, and then were removed by slight substrate deformation or thermal shock treatment. The films were finely cut into the size of 30 mm $\times$ 40 mm and one side was polished to mirror finish. A thin aluminum film was deposited on the polished ZrO_2 films by a physical evaporation method in order to increase optical reflectivity of argon laser in the interferometer. The polished APS, VPS-NiCoCrAlY and APS-ZrO_2 films have typical thickness of 250, 360 and 350 μm, and as-deposited porosity of $14 \pm 2\%$, $10 \pm 2\%$ and $21 \pm 3\%$ measured by laser microscope, respectively. The surface morphologies of the polished specimens are shown in Fig. 1.

TABLE I Plasma spraying conditions for NiCoCrAlTaY and ZrO_2 coatings

Powder	NiCoCrAlY		ZrO_2-8Y_2O_3
Spraying mode	APS	VPS	APS
Working gas Ar/N_2, slpm	30/12	30/12	30/12
Current (A)	350–400	400–450	450–500
Voltage (V)	30–35	30–35	35–40
Powder injection manner	External	External	Internal
Powder feed rate (g/min)	10	10	5
Stand-off distance (mm)	120–140	190–210	100–120
Carrier gas Ar (slpm)	5.5	5.5	4.5

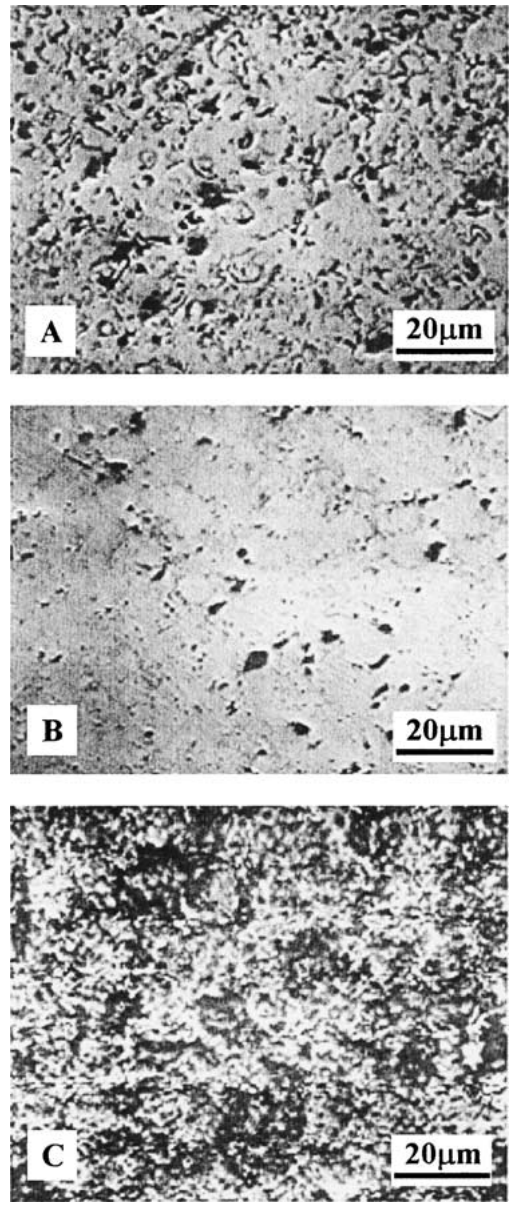

Figure 1 Surface morphologies of the plasma sprayed coatings observed by laser microscope, (A) NiCoCrAlY coating deposited by APS, (B) NiCoCrAlY coating deposited by LPPS, (C) ZrO_2-8%Y_2O_3 coating eposited by APS.

SAWs were generated by adiabatic thermal expansion due to line-focused pulse of a Q-switched Nd : YAG pulse laser (wavelength: 1.06 μm, half-value duration: 5 ns). Out-of-plane displacement induced by SAWs were monitored by a heterodyne-type laser interferometer (frequency bandwidth: 20 KHz–20 MHz, sensitivity: 1×10^8 V/m), digitized by an A/D converter and stored in a personal computer. All the collected data were processed in a workstation. Propagation distance (P.D.) was adjusted by using two 2D and 3D-stages with a spatial resolution of 1 and 2 μm, respectively, and was calibrated experimentally by the Rayleigh velocity of pure aluminum bulk. In the case of Lamb wave measurement, freestanding film specimens were installed in an arrangement of cantilever or suspension. The experimental setup of the laser-induced SAW system is shown schematically in Fig. 2.

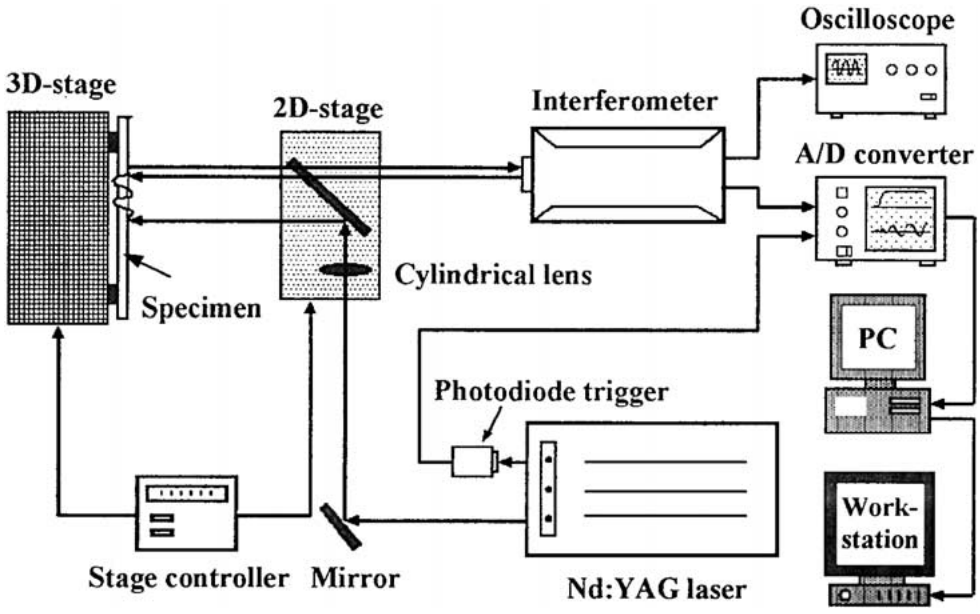

Figure 2 Schematic setup of surface acoustic wave excitation and detection system.

3. Results and discussion

3.1. Evaluation of elastic properties from group velocity dispersions of A_0-Lamb waves

First, antisymmetric mode (A_0-mode) Lamb waves were induced in freestanding NiCoCrAlY and ZrO_2 film specimens while YAG laser beam irradiated on the surface of the films. The signal/noise ratio was increased by a signal averaging technique, and the same measurement was repeated typically 4–6 times by changing measurement locations, for the purpose of examining the experimental reproducibility. Some of the detected waveforms of A_0-mode Lamb waves are presented in Fig. 3. Next, the group velocity dispersions of the measured waves were obtained by wavelet transform as expressed in Equation 1 [21],

$$(W_\psi f)(b,a) = |a|^{-1/2} \int_{-\infty}^{+\infty} \bar{\psi}\left(\frac{t-b}{a}\right) f(t)\,\mathrm{d}t \quad (1)$$

Where $f(t)$ is measured wave function in time domain; a and b are scale and shift parameters, respectively. $a_n = 2^{n/4}$, $b_m = m\Delta t$. Δt is the sampling interval. $\psi(t)$ denotes mother wavelet. The Gabor function is employed as mother wavelet and is given in Equation 2 [22],

$$\psi(t) = \pi^{-1/4}\left(\frac{\omega_p}{\gamma}\right)^{1/2} \exp\left[-\frac{t^2}{2}\left(\frac{\omega_p}{\gamma}\right)^2 + j\omega_p t\right] \quad (2)$$

where the central frequency $\omega_p = 2^{1/2}\pi/\Delta t; \gamma = 5.336$.

The group velocity dispersions of A_0-Lamb waves are shown in Fig. 4. A_0-mode Lamb wave is dispersive, and its group velocity increases with increasing frequency. The measured group velocities were corresponded to the frequency range of 0.3–6.5 MHz, with the maximum error of 20 m/s and 45 m/s for NiCoCrAlY and ZrO_2, respectively.

Elastic properties including Young's modulus E, Poisson's ratio ν, density ρ and thickness, can be estimated by a Simplex-aided inverse analysis as shown in Fig. 5, provided that the estimated materials is isotropic. In order to reduce the uncertainty of the estimation, the thickness values measured by metallography were used as known parameters. In the procedure, a set of initial parameters are given, then the experimental group velocity $V_g(f)$ is compared with the computed velocity dispersion $V_g^*(f)$. Next, the error $|V_g^*(f) - V_g(f)|$, is compared to a convergence condition with the additional restriction of $\Delta E < 1 \times 10^{-3}$ GPa, $\Delta\nu < 1 \times 10^{-4}$ and $\Delta\rho < 1 \times 10^{-2}$ kg/m^3. A set of 12–15V_g data points in the frequency range of 0.3–6.5 MHz is used in the procedure. Unless the error sum satisfies the convergence condition, new initial parameters are provided by Simplex method and the process is repeated until the converging condition is satisfied, when the optimized E, ν and ρ are determined. This process was satisfactory for APS-NiCoCrAlY and ZrO_2, but not for VPS-NiCoCrAlY where a unique solution could not be found with the above estimation processing. As shown in Fig. 6A, there are three solutions respond to the minimum error sum, and the estimated E and ν values of VPS-NiCoCrAlY are in the range of 135–138 GPa and 0.18–0.23, respectively, so the main difficulty of using Simplex method was in determining Poisson's ratio. Therefore, another algorithm was proposed to overcome the problem by supplying sheet velocity C_E,

$$C_E = 2C_T\sqrt{1 - \left(\frac{C_T}{C_L}\right)^2} \quad (3)$$

where C_T and C_L are the transverse and longitudinal bulk wave velocity, respectively.

In the new procedure, the sum error of group velocity is calculated numerically and plotted as a function of C_L or C_T. The optimized C_T (C_L) is specified as 2733 m/s

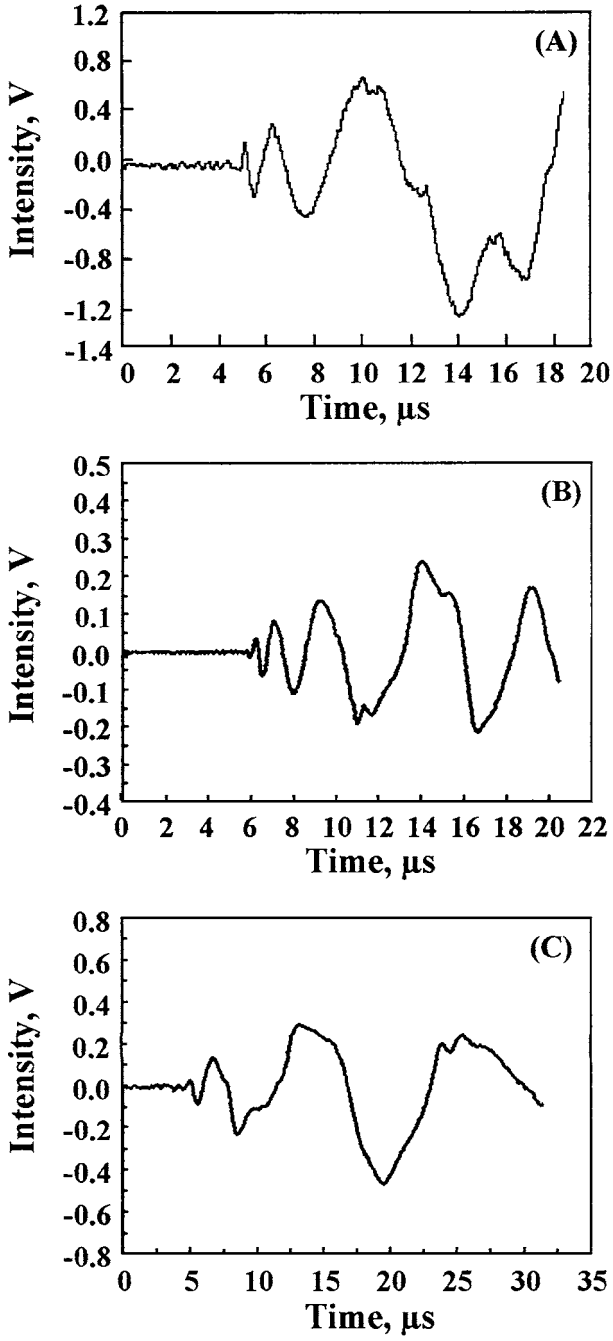

Figure 3 Typical waveforms of A_0-mode Lamb waves in freestanding sprayed specimens, (A) APS-NiCoCrAlY, P.D. = 9.98 mm, (B) VPS-NiCoCrAlY, P.D. = 16.37 mm, (C) ZrO_2-8%Y_2O_3, P.D. = 9.77 mm.

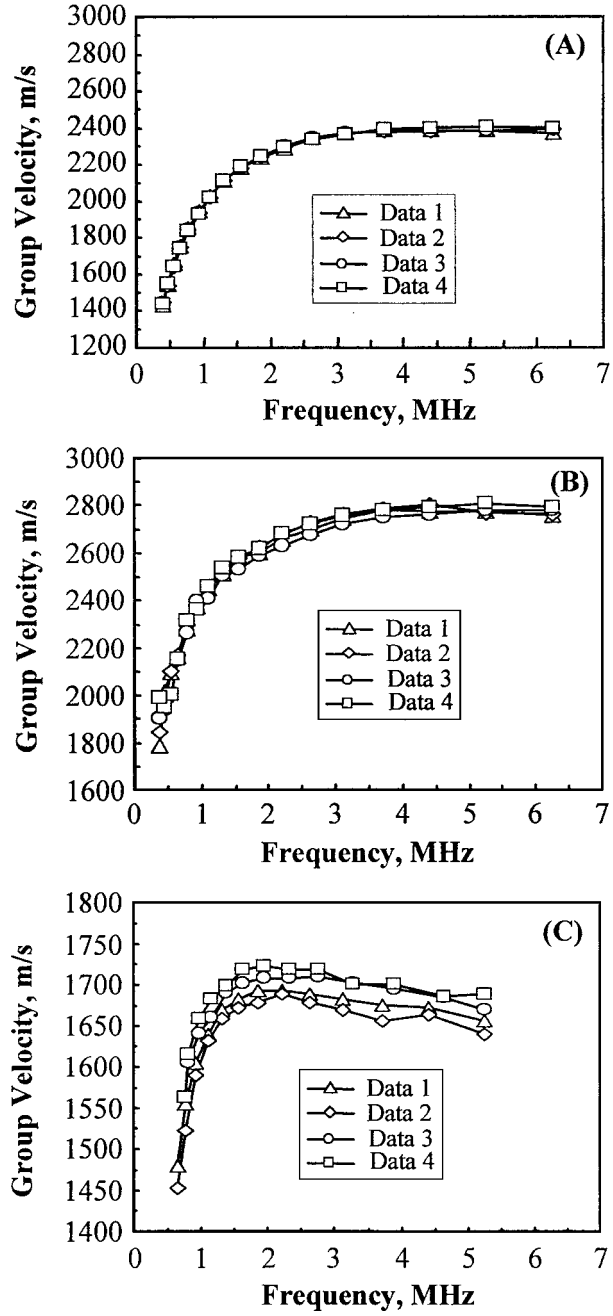

Figure 4 Group velocity dispersions of A_0-Lamb waves excited in freestanding sprayed films by a line-focused YAG laser, (A) NiCoCrAlY deposited by APS, (B) NiCoCrAlY deposited by VPS, (C) ZrO_2-8%Y_2O_3 deposited by APS.

(4835 m/s) from the plotting at the minimum error point as shown in Fig. 6B. Further, the estimated C_T and C_L as well as the measured density 7408 kg/m^3, were used for the evaluation of E and ν from Equations 4 and 5, respectively,

$$E = \frac{\rho C_T^2\left(3C_L^2 - 4C_T^2\right)}{C_L^2 - C_T^2} \tag{4}$$

$$\nu = \frac{C_L^2 - 2C_T^2}{2\left(C_L^2 - C_T^2\right)} \tag{5}$$

The estimated elastic properties of the sprayed materials are given in Table II. Young's modulus of APS-NiCoCrAlY is some 40 GPa lower than that of VPS-NiCoCrAlY, but much higher than that of ZrO_2, about 39 GPa. The reductions in the estimated E and ρ values of the sprayed materials appear to be reasonable due to their defective structures, and the results are consistent with those of NiCrAlY (E = 100–160 GPa) and ZrO_2 (E = 10–50 GPa) investigated in others' studies [3, 5, 6, 26–28].

3.2. Comparison of using S_0 and A_0-mode Lamb waves for elastic property evaluation

Lamb wave contains multi-modes such as symmetric modes (S_i-mode, i = 0, 1, 2, ...) and antisymmetric mode (A_i-mode), and in principle either of the multi-mode waves can be used for elastic property estimation. In this section, we will reveal the restriction of using

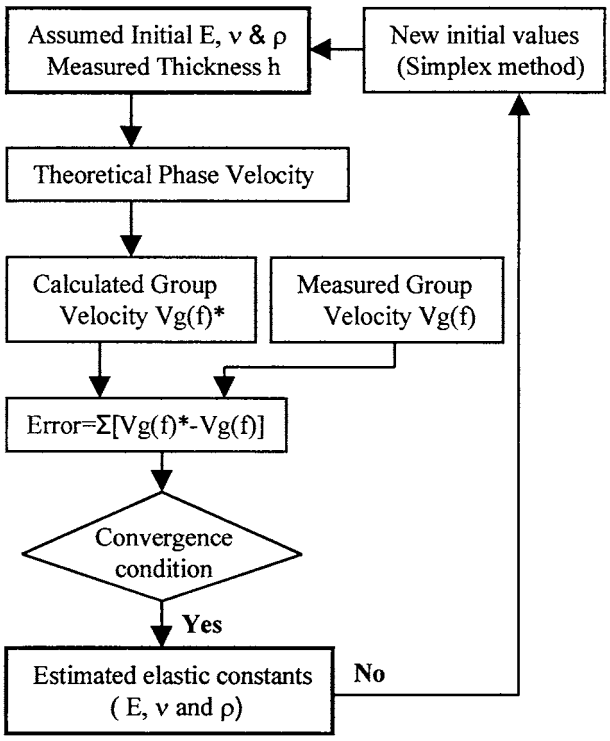

Figure 5 Flow chart for the estimation of elastic properties by a Simplex-aided inverse processing.

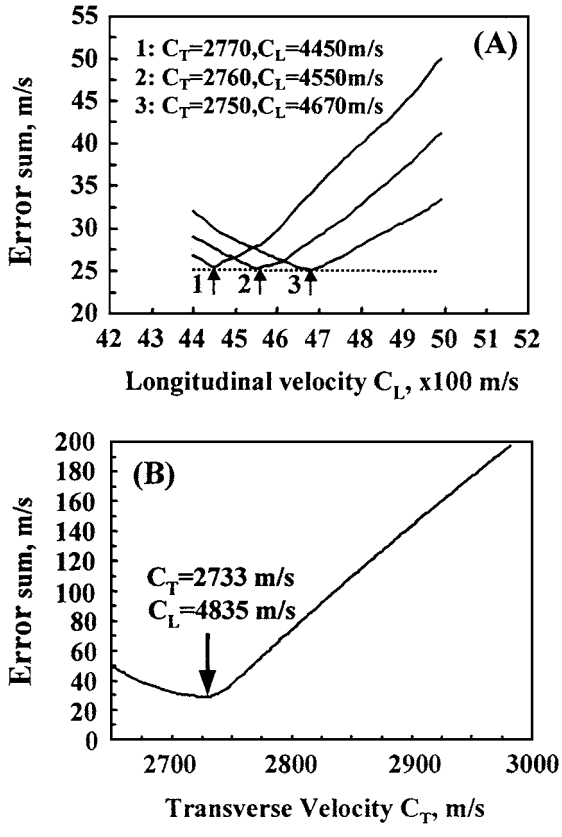

Figure 6 Error sum of group velocity versus C_L/C_T in the procedure of elastic property estimation of VPS deposited NiCoCrAlY, (A) By Simplex-aided inverse analysis, (B) By novel inverse analysis supplying a sheet velocity C_E.

S_0-mode Lamb wave for the estimation of high porosity materials in comparison to using A_0-mode wave.

In the experimental, both S_0- and A_0-mode Lamb waves were generated while YAG laser beam irradiated on the edge of freestanding film specimens, and

TABLE II Comparison of elastic properties of the sprayed and bulk materials

Specimens	Elastic properties		
	Young's modulus (GPa)	Poisson's ratio	Density (kg/m^3)
APS-NiCoCrAlY	101 ± 3	0.24 ± 0.01	7142
VPS-NiCoCrAlY	140 ± 5	0.26 ± 0.02	7408
APS-ZrO_2-8%Y_2O_3	39 ± 3	0.25 ± 0.01	5300
AISI 304 steel [23]	193	0.3	8000
Pure Ni [23, 24]	190	0.3	8902
Sintered ZrO_2-8wt%Y_2O_3 [25]	220	0.3	5920

their waveforms are shown in Fig. 7. The early arriving component is identified as S_0-mode Lamb wave, and the followed one as A_0-mode one. Complete S_0- and A_0-mode waves were generated and monitored in

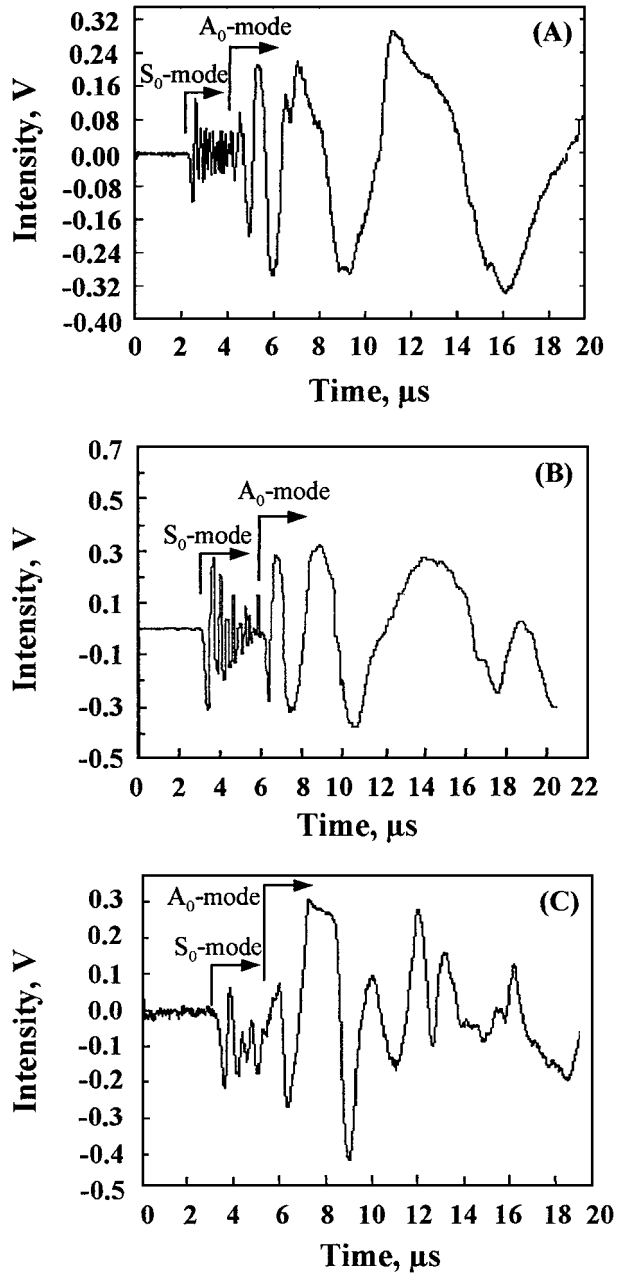

Figure 7 Waveforms of S_0 and A_0-mode Lamb waves generated in free-standing sprayed films, (A) APS-deposited NiCoCrAlY, P.D. = 9.61 mm, (B) VPS-deposited NiCoCrAlY, P.D. = 13.94 mm, (C) APS-deposited ZrO_2-8%Y_2O_3, P.D. = 8.02 mm.

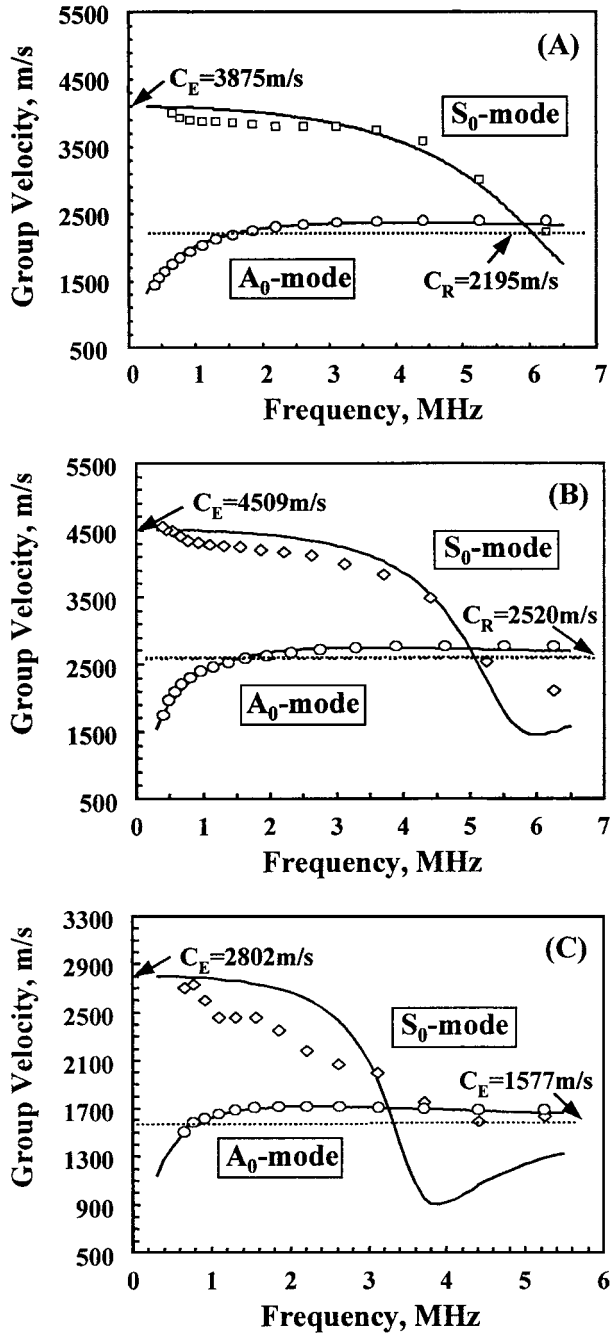

Figure 8 Group velocity dispersions of S_0 and A_0-mode Lamb waves shown in Fig. 7, (A) APS-deposited NiCoCrAlY, (B) VPS-deposited NiCoCrAlY, (C) APS-deposited ZrO_2-8%Y_2O_3.

NiCoCrAlY, but not in ZrO_2, especially for high frequency component of S_0-mode wave. By wavelet transform the group velocity dispersions of S_0 and A_0-mode Lamb waves in the film specimens were obtained and are presented in Fig. 8, in which the experimental and the computed data using the estimated properties in the Section 3.1, are represented by dotted points and solid lines, respectively. It is noticed that the group velocity of A_0-mode wave increases with increasing frequency, but it is inverse for that of S_0-mode wave. Another feature is the velocities of both S_0- and A_0-mode waves tend to the constant Rayleigh velocity C_R at high frequency. In fact, it is quite difficult to determine the velocity of S_0-mode Lamb wave at high frequency such as >5 MHz for NiCoCrAlY and >3.5 MHz for ZrO_2 due to the high acoustic attenuation nature of the sprayed materials with a high porosity. Therefore, the results of elastic property estimation from the S_0-mode velocity dispersions were strongly dependent on how to choose the experimental data points, or even no reasonable result was obtained in the case of ZrO_2. In this experimental, the measured group velocity dispersions of S_0-mode Lamb waves were used to compare with the computed ones by using the elastic properties estimated from A_0-mode Lamb waves, in order to examine the validity of the estimated values in some extend. In Fig. 8, it is evident that the measured and the computed S_0- and A_0-Lamb wave velocities matched well for NiCoCrAlY, but not those of S_0-mode Lamb waves for ZrO_2. Moreover, the S_0-mode velocity at zero frequency is sheet velocity C_E correlating to the fastest arriving wave [29]. The C_E value of VPS-NiCoCrAlY was determined from the S_0-mode Lamb wave and used for the estimation of elastic properties. In Fig. 8C, the fact that the measured C_E from S_0-mode wave in ZrO_2 deposit is close to the computed value, indicates the validity of the estimated properties. Therefore, it is ensured that A_0-mode Lamb wave is more suitable for the elastic property estimation of the porous materials than S_0-mode wave, but the latter can be useful for examining the reliability of the estimated results.

3.3. Rayleigh waves for the estimation of elastic properties

SAWs contain several types of waves including Lamb and Rayleigh waves. Individual Lamb and Rayleigh waves can be generated when their wavelength is greater or smaller than the thickness of tested plate specimen, respectively. Rayleigh wave measurement can be carried out in a coated substrate without removal of the coating, so it is a real nondestructive test technique from the point of sample preparation. In this section, we will discuss the feasibility of using Rayleigh wave velocity dispersions for the evaluation of elastic properties of the sprayed deposits.

Rayleigh waves were excited in the deposits on stainless steel substrates by laser ultrasonic technique. The waveforms of Rayleigh waves excited in VPS-NiCoCrAlY and ZrO_2 are shown in Fig. 9, and their group dispersions are given in Fig. 10, in which the experimental data are represented by dotted points and the theoretical data by solid lines. The theoretical velocities were computed from the estimated elastic properties by Adler's matrix transfer method. The Rayleigh group velocity of steel substrate is nondispersive and measured as 2874 m/s, which is close to the existing value of 2924 m/s in literature. In contrast, dispersive group velocities were obtained for the coated samples. The velocity at zero frequency will be the Rayleigh wave velocity of the substrate and that of the deposit at high frequency. In the case of NiCoCrAlY coated specimen, the experimental and theoretical velocities match very well, and thus demonstrates that the elastic properties of VPS-NiCoCrAlY can be estimated precisely from the Rayleigh wave dispersion by Adler's method as well. The metallographic observation on the cross-sections of the freestanding films have testified that no obvious damages (mainly cracking)

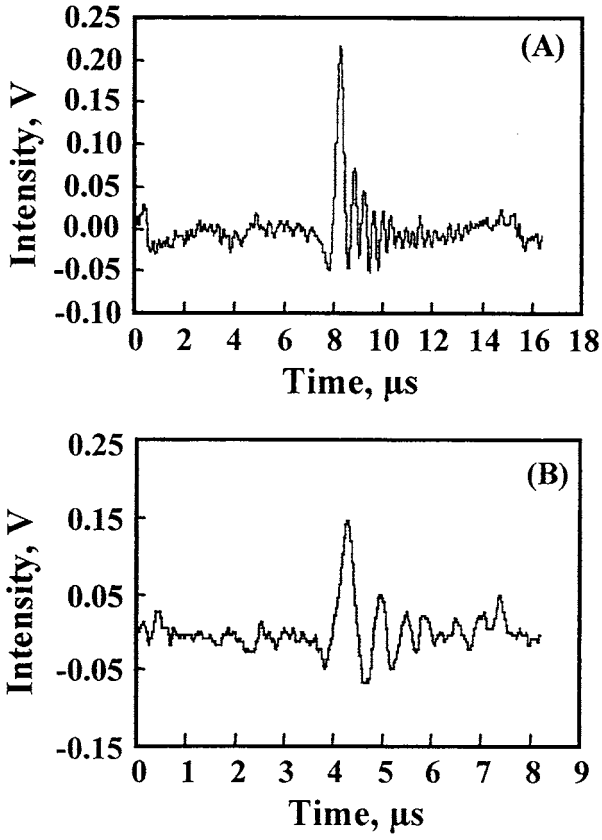

Figure 9 Waveforms of the Rayleigh waves induced in the coatings with steel substrates, (A) VPS-deposited NiCoCrAlY, P.D. = 23.22 mm, (B) APS-deposited ZrO_2-8%Y_2O_3, P.D. = 11.64 mm.

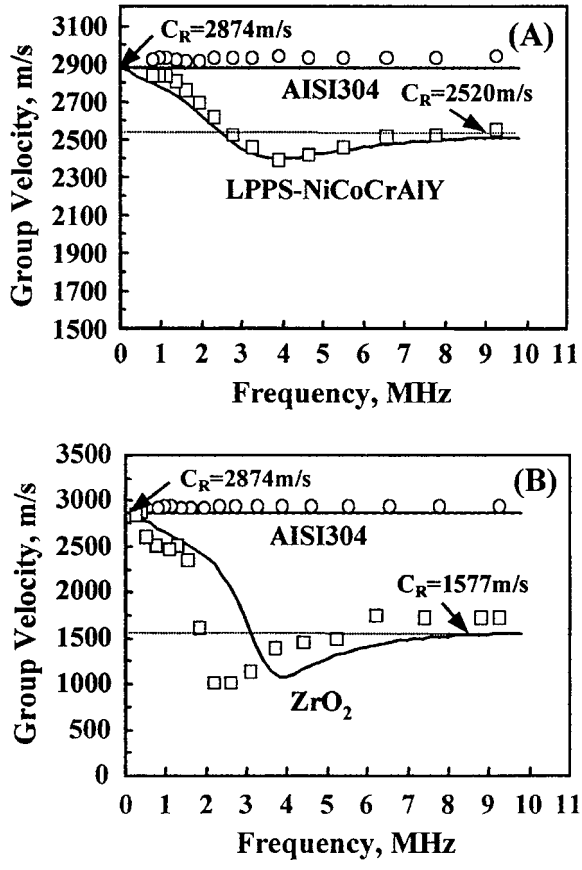

Figure 10 Group velocity dispersions of the Rayleigh waves shown in Fig. 9, (A) VPS-deposited NiCoCrAlY, (B) APS-deposited ZrO_2-8%Y_2O_3.

were induced in the removal procedure of NiCrAlY and ZrO_2 films. The good agreement between the measured and computer data for VPS-NiCrAlY provides additional evidence for no induced damages in free-standing films. In the case of ZrO_2, the deviation in group velocity was substantial in the frequency range of 2–5 MHz and it become very difficult to estimate the elastic properties from the experimental data with an acceptable calculation error. In the estimation procedure by Adler's matrix transfer method, it is assumed that the displacement must be continuous at the interfaces of layered material. From the frequency range the deviation occurred, it was postulated that the continuous displacement condition could not be satisfied due to the weak interface bonding or distinct difference in physical properties of ZrO_2 coating and steel substrate in ZrO_2 coated specimen. Moreover, the high attenuation nature of the porous ZrO_2 deposit may also account for the deviation. Therefore, the application of Rayleigh wave dispersion for the elastic property estimation of a sprayed sample will be limited by interface bonding situation, coating/substrate materials and their acoustic characterization.

3.4. Comparison of elastic properties of sprayed and bulk materials

The elastic properties of two kinds of dense materials, rolled pure nickel foil (200 μm) and sintered yttria (8 wt%) stabilized zirconia foil (250 μm), were evaluated by the same procedure described in the Section 3.1. The Lamb waves excited in the two sheets are shown in Fig. 11. It is noticed that both S_0 and A_0-components of the Lamb waves in the foils are very integral comparing to those in the sprayed films. The group velocity dispersions of Lamb waves were obtained by wavelet transform, and those of A_0-mode Lamb waves were used for the estimation of elastic properties of the dense foils. The estimated properties are listed in Table III. The estimated Young's moduli are 226 GPa for nickel and 241 GPa for zirconia, which are close to the literature values of 190 GPa for bulk nickel and of 220 GPa for YPS-zirconia [23–25]. Further, the theoretical group velocities of S_0 and A_0-mode waves were computed by using the estimated elastic properties and are compared with the experimental data in Fig. 12. The computed data (solid lines) match the experimental data (dotted points) very well for both the dense materials. These results testify that the experimental procedure and the data processing are valid and exact for the elastic constant estimation in the present work.

In comparison to the bulk materials, the sprayed materials have much low elastic stiffness, especially

TABLE III Results of estimated elastic properties of the dense materials

Specimens	Elastic properties		
	Young's modulus (GPa)	Poisson's ratio	Density (kg/m^3)
Rolled pure Ni	226 ± 2	0.29	8750
Sintered YPS-ZrO_2	241 ± 3	0.24	6401

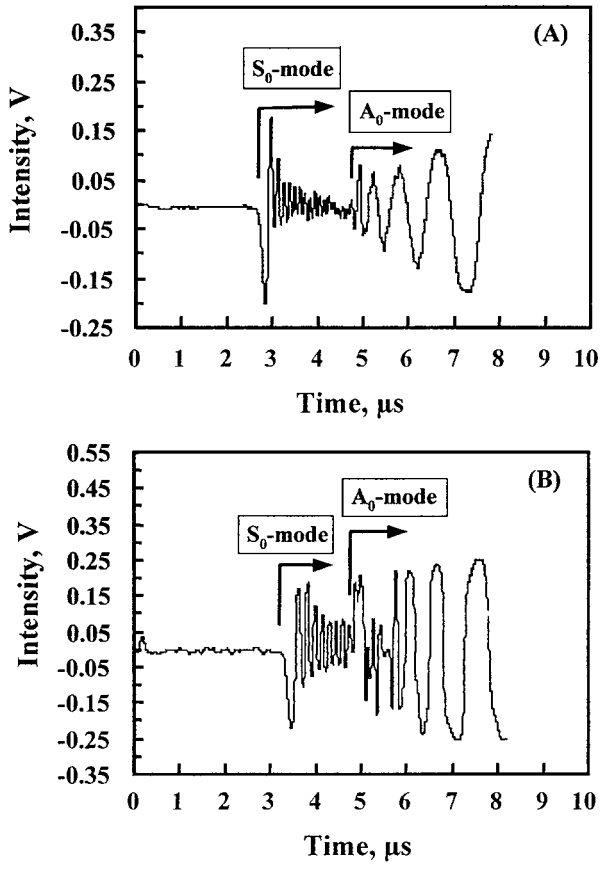

Figure 11 Waveforms of Lamb waves excited in bulk materials, (A) Pure nickel foil, thickness = 200 μm, P.D. = 15.00 mm, (B) Sintered yttria (8 wt%)-zirconia, thickness = 320 μm, P.D. = 22.10 mm.

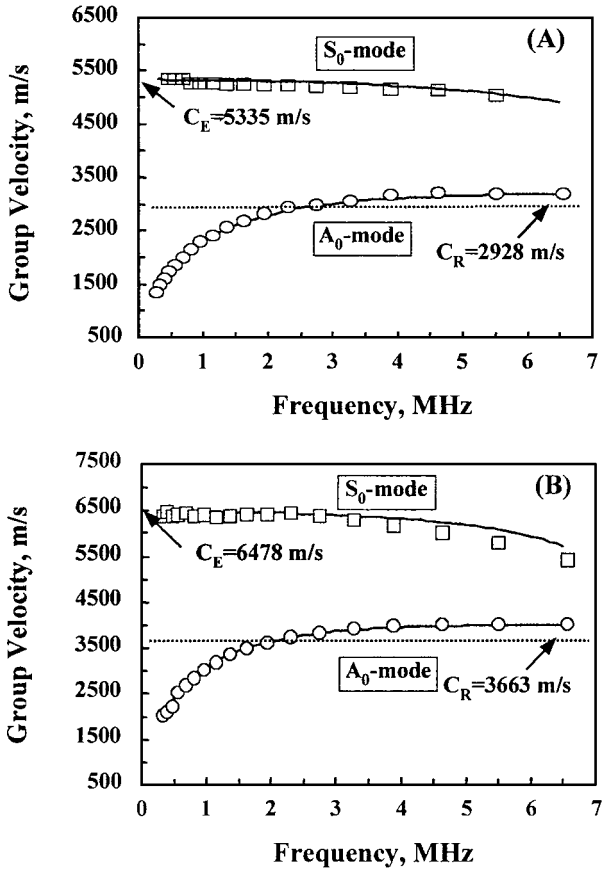

Figure 12 Group velocity dispersions of the Lamb waves shown in Fig. 11. The experimental data are represented by dotted points and the computed data by solid lines. (A) pure nickel foil, (B) Sintered yttria (8 wt%)-zirconia foil.

Young's modulus for the sprayed zirconia. For the case of NiCoCrAlY deposits, the reduced elastic properties can be correlated closely to the presence of porosity. In addition, the lamellar microstructure may also contribute to the reduction in elastic properties due to its effect on reducing the coating integrity. From the literature data on porosity dependency of elastic moduli of sintered zirconia [24], however, it is believed that the significant reduction in elastic modulus of sprayed ZrO_2 should not be attributed to the presence of pores in the deposits. Probably, the results resulted from the presence of micro-cracking network. The micro-cracks as scattering center for acoustic waves will increase significantly acoustic attenuation of the waves propagating in the defective materials. This can also be used to explain the inability of using S_0-mode Lamb wave for estimating the elastic properties of the sprayed ZrO_2 in this study.

4. Conclusions

The elastic properties of plasma sprayed materials have been evaluated by measuring their group velocities of surface acoustic waves (SAWs) excited by laser ultrasonic technique. Different mode SAWs, primarily Lamb and Rayleigh waves, were generated in either freestanding films or in the deposits with substrates, and their advantages and limitation for the evaluation of elastic properties of the sprayed materials were exploited and analyzed. The Main summaries are obtained from the experimental results.

1. Young's moduli of plasma sprayed NiCoCrAlY and ZrO_2 were evaluated as 100–140 GPa and 40 GPa, respectively, which are much lower in comparison to those of the comparable dense materials. The low-porosity NiCoCrAlY produced by vacuum plasma spraying has the highest Young's modulus and density among the tested specimens.

2. Elastic properties of the sprayed deposits have been determined successfully from the group velocity dispersions of A_0-mode Lamb waves excited in freestanding sprayed films. S_0-mode Lamb waves were also applicable to the property estimation of NiCoCrAlY deposits, but not to that of ZrO_2 deposit which is more porous and microcracking-contained.

3. Applicability of Rayleigh waves to elastic property estimation was obviously dependent on the interface integrity and bonding situation in the coated specimens. Reproducible elastic properties of NiCoCrAlYs were obtained from their group velocity dispersions of Rayleigh waves, however, it was incapable of determining the elastic properties of sprayed ZrO_2 from its Rayleigh wave velocity due to the weak interfacial bonding and inconsequent displacement across the interface of ZrO_2 and steel substrate.

Acknowledgement

One of the authors (X. Q. Ma) gratefully acknowledges financial support from the Japan Society for the Promotion of Sciences and the Ministry of Education of Japan. We would like to thank Prof. K. Ono from University of California at Los Angeles for helpful discussion.

References

1. H. D. STEFFENS and U. FISCHER, in "Thermal Spray Technology-New Ideas and Processes," edited by D. L. Houck (ASM International, Materials Park, OH, 1989) p. 167.
2. K. S. SHI, Z. Y. QIAN and M. S. ZHUANG, *J. Amer. Ceram. Soc.* **71** (1988) 924.
3. J. A. THOMSON and T. W. CLYNE, in United Thermal Spray Conference' 99, Dussedorf, May 1999, edited by E. Lugscheider and P. A. Kammer (ASM Thermal Spray Society, Material Park, OH, 1999) p. 835.
4. D. B. MARSHALL, T. NOMA and A. G. EVANS, *J. Amer. Ceram. Soc.* **65** (1982) C175.
5. S. H. LEIGH, C. K. LIN and C. C. BERNDT, *ibid.* **80** (1997) 2093.
6. J. S. WALLACE and J. ILAVSKY, *J. Thermal Spray Technol.* **7** (1998) 521.
7. J. F. W. BELL and J. Y. F. CHEN, *NDT Int.* **14** (1981) 325.
8. H. M. LEDBETTER, S. K. DATTA and R. D. KRIZ, *Acta Metall.* **32** (1984) 2225.
9. T. K. SHEN and P. HING, *J. Mater. Sci.* **32** (1997) 6633.
10. D. A. HUTCHINS, K. LUNDGREN and S. B. PALMER, *J. Acoust. Soc. Am.* **85** (1989) 1441.
11. W. P. ROGERS, *Res. Nondestruct. Eval.* **6** (1995) 185.
12. S. L. BOWLES and C. M. SCALA, *Non-Destructive Testing* **33** (1996) 164.
13. Y. HAYASHI, S. OGAWA, H. CHO and M. TAKEMOTO, *J. NDI (Japan)* **46** (1997) 58.
14. G. SOCINO, N. SPARVIERI, F. TREQUATTRINI and E. VERONA, *Mater. Chem. Phys.* **23** (1989) 464.
15. H. NISHINO, Y. TSUKAHARA, Y. NAGATA, T. KODA and K. YAMANAKA, "Nondestructive Characterization of Materials VI" (Plenum Publishing Corp, New York, USA, 1994) p. 307.
16. H. CHO, H. SATO, Y. TUKAHARA, M. INABA and A. SATO, in Proc. 1995 IEEE Ultrasonic Sym., Seattle, 1995, p. 757.
17. A. ISHIDA, Y. MIZUTANI, M. TAKEMOTO and K. ONO, in 6th Inter. Symp. Acoust. Emiss. Comp. Mater., San Antonio, Taxas, June, 1998, p. 211.
18. R. J. DEWHURST, *Nondestr. Test Commun.* **1** (1983) 93.
19. D. A. HUTCHINS and D. E. WIKINS, *J. App. Phys.* **58** (1985) 2469.
20. D. SCHEIDER and D. TUCKER, *Thin Solid Films.* **290/291** (1996) 305.
21. R. KRONKAND-MARTINET, J. MORLET and A. GROSSMANN, *Int. J. Pattern Recognition Art Int.* **1** (1989) 273.
22. D. GABOR, *J. Inst. Electr. Eng.* **93** (1946) 429.
23. J. R. DAVID *et al.* (eds.), Metal Handbook, 10th ed. Vol. 1 (ASM International, Materials Park, OH, 1990).
24. A. J. A. WINNUBST, K. KEIZER and A. J. BURGRAAF, *J. Mater. Sci.* **18** (1983) 1958.
25. R. P. INGEL and D. L. LEWIS III, *J. Amer. Ceram. Soc.* **71** (1988) 265.
26. P. A. SIMERS and W. B. HILLIG, NASA-CR-165351, 1982.
27. L. S. COOK, A. WOLFENDEN and W. J. BRINDLEY, *J. Mater. Sci.* **29** (1994) 5104.
28. R. S. LIMA, A. KUCUK and C. C. BERNDT, in Thermal Spray: Surface Engineering via Applied Research, Montreal, May 2000, edited by C. C. Berndt (ASM International, Material park, OH, 2000) p. 1201.
29. R. J. DEWHURST, C. EDWARDS, A. D. WHEKIE and S. B. PALMER, *J. Appl. Phys. Lett.* **51** (1989) 1066.

Received 17 August 2000
and accepted 7 May 2001